Biosensors and Bioelectronics 85 (2016) 657–663

Contents lists available at ScienceDirect

Biosensors and Bioelectronics

journal homepage: www.elsevier.com/locate/bios

Pt@AuNPs integrated quantitative capillary-based biosensors for point-of-care testing application

Ze Wu [a,1], Qiangqiang Fu [a,1], Shiting Yu [a], Liangrong Sheng [b], Meng Xu [b], Cuize Yao [a], Wei Xiao [a], Xiuqing Li [a], Yong Tang [a,c,*]

[a] Department of Bioengineering, Guangdong Province Key Laboratory of Molecular Immunology and Antibody Engineering, Jinan University, Guangzhou 510632, PR China
[b] Oncology Department of the First Affiliated Hospital of Jinan University, Guangzhou 510632, PR China
[c] Institute of Biotranslational Medicine, Jinan University, Guangzhou 510632, PR China

ARTICLE INFO

Article history:
Received 13 December 2015
Received in revised form
6 May 2016
Accepted 23 May 2016
Available online 24 May 2016

Keywords:
Capillary-based biosensor
Core-shell Pt@Au nanoparticle
Point-of-care testing
Prostate-specific antigen
Carcinoembryonicantigen

ABSTRACT

Current diagnostic technologies primarily rely on bulky and costly analytical instruments. Therefore, cost-effective and portable diagnosis tools that can be used for point-of-care tests (POCT) are highly desirable. In this study, we report a cost-effective, portable capillary-based biosensor for quantitative detection of biomarkers by the naked eye. This capillary-based biosensor was tested by measuring the distance of blue ink movement, which was directly correlated with the oxygen (O_2) produced by efficient core-shell Pt@Au nanoparticles (Pt@AuNPs) catalysts decomposed hydrogen peroxide (H_2O_2). By linking the Pt@AuNPs with antibodies, capillary-based biosensor sandwich immunoassays were constructed. The concentrations of the target proteins were positively correlated with the distances of ink movement. To demonstrate their performance, the biosensors were used to detect the cancer biomarker sprostate-specific antigen (PSA) and carcinoembryonic antigen (CEA). The linear detection range (LDR) of the capillary-based biosensor for detecting PSA was from 0.02 to 2.5 ng/mL, and the limit of detection (LOD) was 0.017 ng/mL. LDR of the biosensor for detecting CEA was from 0.063 to 16 ng/mL, and the LOD was 0.044 ng/mL. For detection of PSA and CEA in clinical serum samples, the detection results of the capillary-based biosensor were well correlate with the results from of chemiluminescence immunoassays (CLIAs). Thus, the capillary-based biosensor may potentially be a useful strategy for point-of-care testing, in addition to being portable and cost effective.

1. Introduction

The healthcare field is currently facing enormous challenges. Accurate and timely diagnoses of diseases have the potential for saving vital time in determining the appropriate treatment, especially in life-threatening conditions. Conventional diagnostic technologies, such as enzyme-linked immunosorbent assays (ELISAs) (Moody et al., 2001), chemiluminescence immunoassays (CLIAs) (Tanaka and Matsunaga, 2000), electrochemical immunoassays (Tang et al., 2007), electrochemiluminescence immunoassays (ECLIs) (Wang et al., 2012), and protein chip assays (Wang et al., 2012), have high sensitivity and high specificity. However, these diagnostic methods rely on bulky and costly analytical instruments and require specialized training. Therefore, cost-effective, compact and accurate diagnostic tools that can be used as point-of-care testing (POCT) devices are highly desirable.

One of the most widely used POCT devices is immunochromatographic sensor, such as colloidal gold-based immunochromatographic sensors (Chen et al., 2015; Hou et al., 2015), due to their ease of use, portability, cost-effectiveness and easily visualized results. When coupled with high-efficiency tracers, such as fluorescent nanoparticles (Fu et al., 2013; Shi et al., 2015), quantum dots (Li et al., 2012), enzymes (Qin et al., 2015) and coded SERS nanoparticles (Fu et al., 2015; Liang et al., 2014), these immunochromatographic sensors can be used for quantitative detection with high sensitivity and accuracy. However, to obtain quantitative results, these devices require expensive equipments. Other products widely used in POCT devices include microfluidic chips (Gervais et al., 2011; Ghannad-Rezaie et al., 2012). Microfluidic chips have the potential to revolutionize clinical diagnoses

* Corresponding author at: Department of Bioengineering, Guangdong Province Key Laboratory of Molecular Immunology and Antibody Engineering, Jinan University, Guangzhou 510632, PR China.
E-mail address: tyjaq7926@163.com (Y. Tang).
[1] These authors contributed equally to the manuscript.

http://dx.doi.org/10.1016/j.bios.2016.05.074
0956-5663/

and personalized therapies due to these could offer quantitative, high-throughput, rapid results and are affordable and portable. However, in practice, microfluidic chips require costly fluid-introducing accessories and pump control systems and result reading instruments, such as fluorescence or optical absorption readers, mass spectrometers or electrochemical or glucose meters, to yield quantitative results (Song et al., 2012). These practical barriers limit the application of microfluidic chips for clinical and personal use widely. Recently, the Qin and Yang research groups have designed elegant multiplexed volumetric bar-chart chips (V-Chips) for quantitative POCT diagnostics (Li et al., 2015; Song et al., 2013, 2014, 2012; Zhu et al., 2014). These methods can be used for quantitative measurement of target proteins and biomarkers.

Based on these considerations, a lower-cost, more portable and more easily used capillary-based quantitative biosensor was developed in our study. This biosensor used general sandwich immunoassay with antibody-coated magnetic beads (MBs) and antibody-coated Pt@AuNPs to detect prostate-specific antigen (PSA) and carcinoembryonicantigen (CEA). In detection of positive samples, mAb1-Pt@AuNPs was bound to mAb2-MBs through antigen bridge effect, after be washed and added H_2O_2, large volume of O_2 was generated. In detection of negative samples, no mAb1-Pt@AuNPs were bound to mAb2-MBs without antigen, after be washed and added H_2O_2, nearly no O_2 was generated. The concentrations of these biomarkers were calculated by measuring the movement distance of blue ink as induced by the production of O_2 via Pt@AuNPs-catalyzed decomposition of H_2O_2. The target protein concentrations were positively correlated with the moving distance of the blue ink (Fig. 1). In the detection of PSA and CEA for clinical serum samples, the results of the capillary-based biosensor were well correlated with those of commercial chemiluminescence immunoassays (CLIAs). Because of its low-cost, user-friendly operation and simple fabrication, capillary-based biosensors have good potential as POCT devices, especially in resource-limited areas.

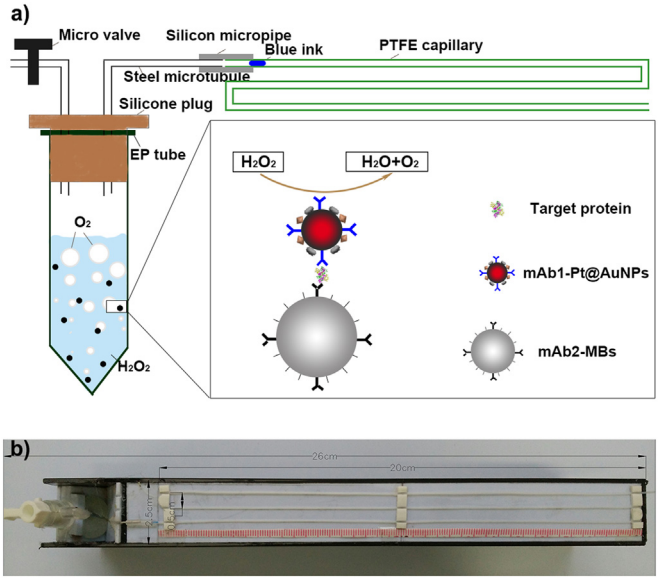

Fig. 1. Principle of the capillary-based biosensor. (a) Schematic illustration of a typical capillary-based biosensor. For detecting positive samples, MB-mAbs first captured the target antigens, then Pt@AuNP-mAbs was combined with the complex, and the Pt@AuNPs catalyzed H_2O_2 to generate O_2, thereby forward-displacing the blue ink within the capillary; For detecting negative samples, Pt@AuNP-mAbs cannot be combined with MB-mAbs, therefore did not produce O_2, which cannot promote the blue ink. (b) Picture of a single-channel device. (For interpretation of the references to color in this figure legend, the reader is referred to the web version of this article.)

2. Materials and methods

2.1. Chemicals and materials

Chloroauric acid ($HAuCl_4 \cdot 3\ h_2O$), Chloroplatinic acid ($H_2PtCl_6 \cdot 6H_2O$), PVP 40,000, streptavidin, catalase and Tween-20 were obtained from Amresco (USA). Bovine serum albumin (BSA), horseradish peroxidase (HRP), CK-MB, α-fetoprotein (AFP), prostate specific antigen (PSA) and carcinoembryonicantigen (CEA) were purchased from Sigma-Aldrich. Trisodium citrate was purchased from Damao reagent (Tianjin, China). N-Hydroxysuccinimide activated MBs (NHS-MBs) with a diameter of 1 μm were purchased from Shanghai Beaver Biological Technology Co., Ltd. (Shanghai, China). Monoclonal antibodies for PSA and CEA were obtained from Shanghai Lingchao Biological Technology Co., Ltd (Shanghai, China). Serum samples associated with PSA were collected from the Department of Laboratory Medicine, Guangdong No. 2 Provincial People's Hospital (Guangzhou, China). Serum samples associated with CEA were collected from the Cancer Center of the First Affiliated Hospital of Jinan University (Guangzhou, China). Hydrogen peroxide (H_2O_2, 30 wt%), Coomassie brilliant blue (CBB) G-250, methyl blue and other commonly used reagents were purchased from GZ Chemical Reagent (Guangzhou, China). Steel microtubules (Ø 0.4 mm*0.15 mm), polytetrafluoroethylene (PTFE) capillaries (Ø 0.3 mm*0.2 mm), fluorinated ethylene propylene (FEP) capillaries (Ø 0.3 mm*0.2 mm), silica micropipe (Ø 0.6 mm*0.3 mm), silica capillaries (Ø 0.3 mm*0.2 mm), silica gel plugs (Ø 5 mm), and miniature valves (Ø 2 mm) were purchased from Pureshi (Shanghai, China). Melt adhesive (EVA Hot Glue, a plastic binder that changes in the physical state of the binder over a range of temperatures.) and a melt adhesive gun were bought from Dremel (Nantong, China). Cutter knife, Small electric drill, acrylonitrile butadiene styrene(ABS) plates special glue (a vinyl polymer as the main body, one-component solvent-based ABS plastic s ABS plastic special glue) were obtained from Crab Kingdom Technology Co., Ltd. (Shenzhen, China).

2.2. Apparatus

Microplate reader (Bio-Tek Instruments, Inc.), transmission electron microscope (TEM, PHILIPS, Holland), and a centrifuge (Beckman, Germany) were used. Ultrapure water (Milli-Q grade, Millipore) with a resistivity of 18.2 MΩ/cm was used throughout this study.

2.3. The reaction system

2.3.1. Preparation of mAb1-Pt@AuNPs

Thirteen-nanometer gold nanoparticles (AuNPs) were synthesized according to a previously reported method (Liu and Lu, 2006) with slight modifications. Typically, 100 mL ultrapure water in a conical flask was heated to boil with vigorous stirring, and 1 ml 1% $HAuCl_4$ solution was added, after boiling again, 1 mL of 1% trisodium citrate was added rapidly and kept stirring over a period of 10 min. Gradually, the color of the solution changed from light yellow to purple and finally to a wine-red color. Stop heating and keep stirring, the resultant AnNPs were stored in 4 °C after cooling to room temperature. Core-shell Pt@Au nanoparticles (Pt@AuNPs) were synthesized (Li et al., 2006) as follows: 200 μL 3.86 mM H_2PtCl_6 was added to 10 mL AuNPs. The mixture was heated to 80 °C under magnetic stirring, and 400 μL aliquot of 10 mM ascorbic acid was slowly added drop wise into this mixture over 3 min with a syringe pump. Afterward, the mixture was heated and stirred for an additional 30 min The diameters of the obtained Pt@AuNPs were determined via TEM to be approximately 16 nm. A

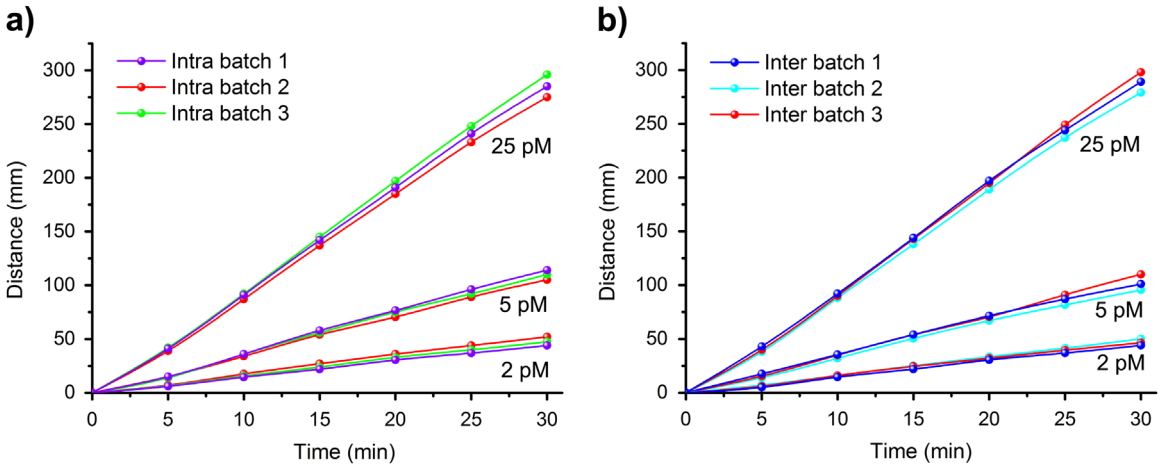

Fig. 2. Stability of the capillary-based biosensors. (a) Movement distances of blue ink with different concentrations of Pt@AuNPs for a single capillary-based biosensor (three trials). (b) Movement distances of blue ink with different concentrations of Pt@AuNPs for three capillary-based biosensors. (For interpretation of the references to color in this figure legend, the reader is referred to the web version of this article.)

specific amount of 1 mg/mL detecting mAb1 was mixed with 1 mL Pt@AuNPs in PBS buffer at pH 6.5. The mixture was kept at room temperature (RT) for 1 h. Next, 100 μL blocking buffer was added to block the surface of the Pt@AuNPs, and the unconjugated mAb1s were removed via centrifugation. Finally, the antibody-conjugated Pt@AuNPs were suspended in 500 μL of 10 mM PBS solution (pH 7.2) and stored at 4 °C.

2.3.2. Preparation of mAb2-MBs

One hundred microliters of MBs was washed with 1 mL washing buffer and suspended in 1 mL PBS. Capturing mAb2s were diluted to 1 mg/mL using 100 mM MES (pH 4.8); this dilution was added to the other MBs preparation. After 2 h, 100 μL of 3 M ethanolamine at pH 9.0 was added, and the mixture was reacted in a rotary mixer for an additional 1 h. The unconjugated mAb2s were removed by using a magnetic rack. The resultant mAb2-MBs were suspended in 1 mL PBS and stored at 4 °C.

2.3.3. Sandwich immunoassays for PSA and CEA

PSA was diluted to different concentrations with PBS buffer (0.01 M, pH 7.4). Then, specific volumes of mAb2-MBs were added to 150 μL of the different concentrations of PSA. The mixtures were reacted in a rotary mixer for 30 min Magnets were used to separate and remove the supernatants, which were re-suspended in 200 μL PBST (0.1% Tween-20 in 0.01 M, pH 7.4 PBS) and collected again to wash away any excess PSA. This washing process was performed 3 times. The mixtures were then re-suspended with 148 μL PBS and incubated with 2 μL of mAb1-Pt@AuNPs for 30 min. After being washed 5 times, the reaction complexes were stored in PBS. The same procedures were used for the CEA immunoassays.

2.4. The read-out system

2.4.1. Device assembly

Our detection device was assembled from acrylonitrile butadiene styrene (ABS) plates. Two parallel steel microtubules were inserted into silica gel plugs to seal the reaction tubes and were fixed on one end of the ABS skeleton. One of the steel microtubules was connected to a miniature valve, and the other one was linked with a polytetrafluoroethylene (PTFE) capillary through a silicone micropipe. Several small pieces of the ABS material were pasted on the observation panel to form card slots and fix the PTFE capillary. The materials for manufacturing the device were shown in Fig. S1.

2.4.2. Signal generation and reading

After the immunoreactions, 300 μL of 30% H_2O_2 was added to the EP tube and quickly agitated. Then, the EP tube was connected to the silicone plug on a readout device, and the micro valve was opened for 5 min after the addition of H_2O_2. Subsequently, the micro valve was shut, and the moving distance of the blue liquid in the PTFE capillary was recorded every 5 min.

2.5. Analytical procedure for clinical samples

The PSA and CEA serum samples were measured by using the capillary-based biosensor with the above-described procedure. If the concentrations of the detected biomarkers were greater than the linear detection range of the capillary-based biosensor, the serum samples were diluted by a factor of 10 and reanalyzed.

3. Results and discussion

3.1. Stability of the read-out device

To assess the stability of the device, the movement distances of the blue ink were recorded every 5 min after reaction (Fig. 2). For investigation of the intra batch variation, the same device was tested for three times sunder the same experimental conditions (Fig. 2(a)). For investigation of the inter batch variation, the same sample was tested with three parallel devices (Fig. 2(b)). There were no obvious diversity for intra and inter batch. Additionally, we found that the capillary material and the composition of the blue ink influenced the stability of the device. Different capillary materials (silica, FEP and PTFE) and inks comprising different substances (alcohol-diluted CBB G-250 and ultrapure water-diluted methyl blue) were tested (Fig. S2). We selected the PTFE capillary and alcohol-diluted CBB G-250 for further tests. The whole device was assembled with ABS, special glue and melt adhesives. Because of the wide availability of the materials and the ease of manufacturing, the entire device was low in cost, and the cost of all materials was less than 0.7 dollars.

3.2. Characterization of Pt@AuNPs

Recent studies have reported that Pt@AuNPs have the ability to efficiently catalyze H_2O_2 to generate O_2 (Zhu et al., 2014). The synthesized Pt@AuNPs had good dispersion and uniform particle size and the surfaces of the particles had regular petal-shaped

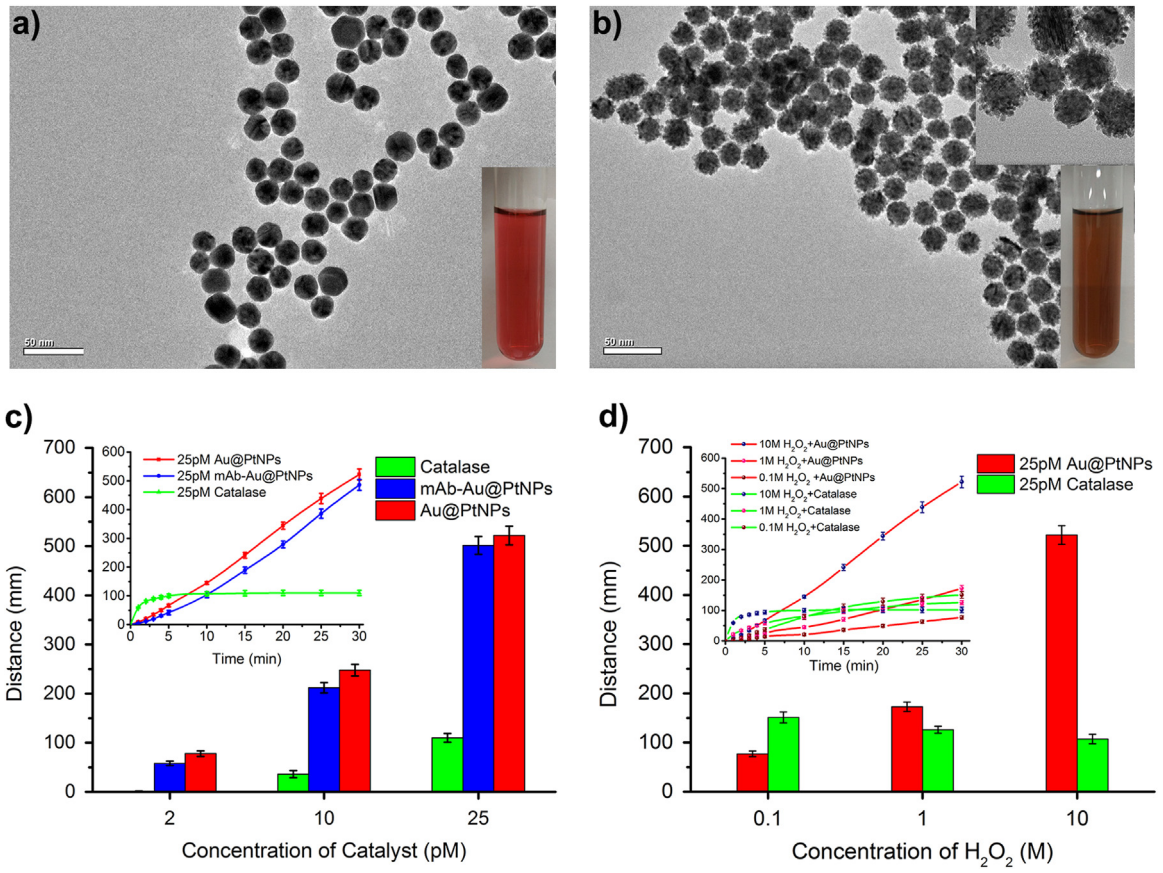

Fig. 3. Characteristic catalytic effects of Pt@AuNPs. (a) TEM images of AuNPs and image of AuNP solution. (b) TEM images of Pt@AuNPs and image of Pt@AuNPs. (c) Catalytic effects for different concentrations of H_2O_2 solution for 25 pM catalase, Pt@AuNPs and mAb-Pt@AuNPs. (d) Catalytic effects for different concentrations of catalase and Pt@AuNPs in 10 M H_2O_2.

protrusions (Fig. 3(a) and (b)). UV–vis spectra of AuNPs and Pt@AuNPs shown in Fig. S3, AuNPs displayed strong optical absorption near 520 nm, whereas the absorbance of Pt@AuNPs decreased at 520 nm and increased from 570 nm to 580 nm. These results indicated that the Pt@AuNPs were synthesized successfully.

The catalytic properties of Pt@AuNPs were studied. We demonstrated the catalytic effect of different concentrations of enzymes and Pt@AuNPs in 10 M H_2O_2 in triplicate (Fig. 3(c); Fig. S4 (A)). To three EP tubes were added 297 μL H_2O_2, 3 μL of 2.5 nM, 1 nM or 0.2 nM of ultrapure water-diluted catalase solutions. The tubes were then connected to the readout device, and the microvalve was shut immediately. The EP tubes were subsequently shaken. For each catalyst, the reaction was monitored by taking pictures every minute for the first 5 min and every 5 min from 5 to 30 min (Fig. S4 (B)). When the concentration of catalase was less than 2 pM, the generated O_2 was not sufficient to move the liquid drop. The moving distance of the blue ink increased as the catalase concentration increased over 2 pM, but the droplet was no longer moving after a certain period of time. Then, we used Pt@AuNPs to perform the same catalytic experiments. Surprisingly, even the concentration was low as 2 pM, catalytic effects and ink movement were observable. Moreover, the Pt@AuNPs steadily catalyzed H_2O_2 to generate O_2 over a prolonged period of time, thereby indicating the excellent stability of the Pt@AuNPs. To evaluate the effects of labeling the Pt@AuNPs with antibodies, we performed another groups of experiments with monoclonal antibody-labeled Pt@AuNPs (mAb-Pt@AuNPs) (Fig. S4 (C and D)). The data shown that the catalytic activity of mAb-Pt@AuNPs did not significantly decrease versus Pt@AuNPs.

We also studied the catalytic performances of catalase and Pt@AuNPs for different concentrations of H_2O_2 (Fig. 3(d)). With highly concentrations of H_2O_2, the Pt@AuNPs had higher and more stable catalytic performances than catalase. At low H_2O_2 concentrations, the catalytic performance of the Pt@AuNPs was less than that of catalase in the short term. However, as the reactions proceeded, the catalytic activity of the Pt@AuNPs gradually exceeded that of catalase (Fig. S4 (E and F)). Additionally, to demonstrate the stability of Pt@AuNPs, we stored catalase and the Pt@AuNPs at room temperature and measured their activities once every week for 8 weeks (Fig. S5). The results demonstrated that the activity of catalase rapidly decreased, and the activity of the Pt@AuNPs remained stable over time. These proved that the Pt@AuNPs have high catalytic efficiency and good stability.

3.3. Measurement of PSA and CEA by using the capillary-based biosensor

To enhance the performance of this biosensor, the amounts of monoclonal antibodies (mAb) labeled Pt@AuNPs and MBs were optimized (Fig. S6). Four microliters of 1 mg/mL anti-PSA mAb1 or 5 μL of 1 mg/mL anti-CEA mAb1 was used for labeling 1 mL Pt@AuNPs; similarly, 8 μL of 1 mg/mL anti-PSA mAb2 or 10 μL of 1 mg/mL anti-CEA mAb2 was used to label 100 μL MBs. Then, effects of the mAb1-Pt@AuNPs and mAb2-MBs addition on properties of this biosensor were study (Fig. S7). The results indicated that 2 μL mAb1-Pt@AuNPs and 6 μL mAb2-MBs were the optimal addition amounts for detecting PSA and CEA, respectively. To reduce nonspecific reactions, we optimized the blocking buffer for mAb1-Pt@AuNPs (Fig. S8).

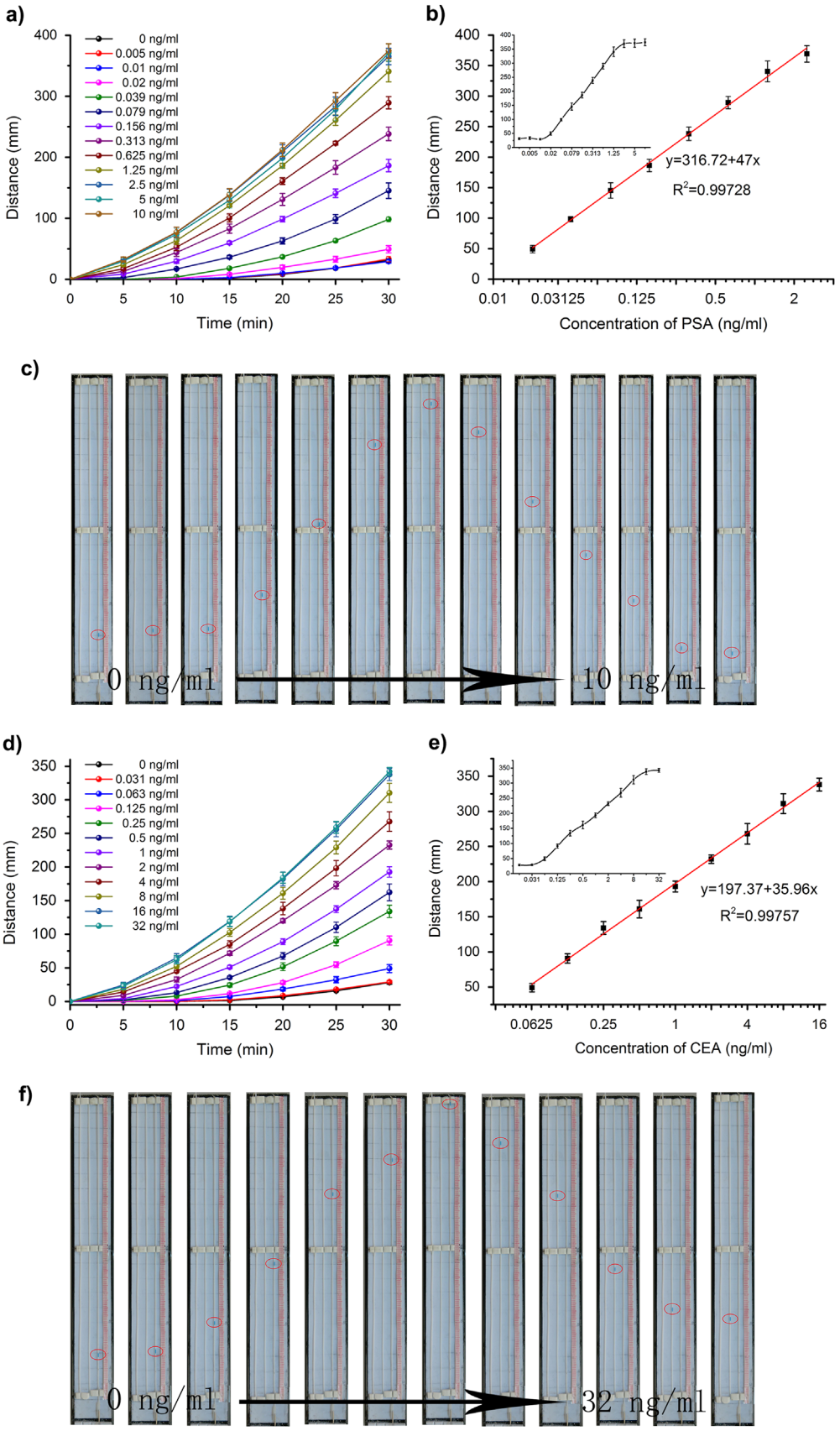

Fig. 4. Detection of PSA and CEA used the capillary-based biosensor. (a) Droplet moving distances for different concentrations of PSA. (b) Linear standard curves of the capillary-based biosensor for PSA. (c) Actual read-outs of PSA samples at 30 min. (d) Droplet moving distances for different concentrations of CEA. (e) Linear standard curves of the capillary-based biosensor for CEA. (f) Actual read-outs of CEA samples at 30 min. Each value represents the mean of three independent experiments (n=3).

A mixed blocking buffer solution consisting of BSA, PVP 40,000 and PEG 4000 was used to block the mAb1-Pt@AuNPs.

We used the capillary-based biosensor to detect PSA and CEA in PBS buffer. Ten microliters of different concentrations of PSA, from 0 ng/mL to 10 ng/mL, were used. As shown in Fig. 4(a–c), as the concentration of PSA increased, the movement distance of the ink increased. In additional, as the H_2O_2 reaction time increased, the movement distance of the ink increased, too. Standard curves from different H_2O_2 reaction time of 10 min, 20 min, 30 min, 45 min and 60 min were established (Fig. S10). Standard curve from 30 min shown better correlation coefficient ($R^2=0.9984$) than others, and the linear dynamic range, sensitivity and background were appropriate and acceptable. Thus we selected 30 min as the H_2O_2 reaction time. When the PSA concentration was 0 ng/mL, the ink movement distance was 31 mm, and the standard deviation (S.D.) was 2.5 mm. When the PSA concentration was 10 ng/mL, the ink movement distance was 374.3 mm, and the S.D. was 11.9 mm. The ink movement distance was used to quantitatively measure the concentration of PSA. A good linear correlation ($R^2=0.998$) between the ink movement distance and the PSA concentration was obtained within the range of 0.02–2.5 ng/mL. The LOD of the capillary-based biosensor was calculated on the basis of the concentration response to the ink movement distance (63 mm-3*S.D.) and was found to be 0.014 ng/mL. The detection principle of the CEA was same as that for the PSA. Ten microliters of different concentrations of CEA from 0 ng/mL to 32 ng/mL were used (Fig. 4 d–f). The LOD of the capillary-based biosensor for detecting CEA was 0.044 ng/mL. The biosensor could detect a wide linear range from 0.063 ng/mL to 16 ng/mL. In comparison to other methods, the developed capillary-based biosensor meets clinical sensitivity demands and is more portable and cost-effective.

3.4. Selectivity of the capillary-based biosensor

To demonstrate the selectivity of the capillary-based biosensor for PSA detection, several common proteins, such as CEA, bovine serum albumin (BSA), horseradish peroxidase (HRP), CK-MB and α-fetoprotein (AFP), were investigated. The distances of the blue ink movement were nearly negligible when 1 ng/mL of CEA, BSA, HRP, CK-MB and AFP were used (Fig. S9 (A)). PSA, BSA, HRP, CK-MB and AFP were used to demonstrate the selectivity of the capillary-based biosensor for CEA detection. The results are shown in Fig. S9 (B). Negligible distances of the blue ink movement were observed from 1 ng/mL of PSA, BSA, HRP, CK-MB and AFP. These results demonstrated the extraordinary selectivity of the capillary-based biosensor.

3.5. Detection of clinical samples

Application of the proposed capillary-based biosensor for the detection of PSA and CEA in serum samples was investigated. Nine serum samples of PSA and sixteen serum samples of CEA were assayed. Usually, serum PSA and CEA levels of patients are above 4.0 ng/mL and 5.0 ng/mL respectively. For matching the linear detection range (LDR) of the sensors, the serum samples were diluted 10 times prior to analysis. The results obtained by this method were compared with those obtained by the commercially available chemiluminescence immunoassays (CLIAs). The results from these two methods exhibited excellent correlations and non-significant differences (Fig. 5). Indicated the biosensor is an effective tool for clinical diagnosis.

4. Conclusions

In summary, a capillary-based biosensor that used gas volume measurements to enable portable, low-cost and instrument-free, especially quantitative detection of clinical samples was developed. Cancer biomarkers PSA and CEA were detected by the biosensor. For detecting PSA, LDR was 0.02–2.5 ng/mL and LOD was 0.017 ng/mL. For detecting CEA, LDR was 0.063–16 ng/mL and LOD was 0.044 ng/mL. The capillary-based biosensors were also used to detect PSA and CEA in serum samples and shown that results were consistent with results from routine clinical diagnostic method, CLIAs. Comparing many traditional diagnostic methods, the capillary-based biosensor has a number of advantages. First of all, this device meets the basic requirements for POCT, including affordability, sensitivity, specificity, ease of use, rapid and robust operation, low equipment requirements, and deliver ability to the end user (termed “ASSURED” by the World Health Organization) (Urdea et al., 2006). In particular, the capillary-based biosensor is simply designed and easy to assemble, this device have the lower cost than most traditional detection methods, yet it may provide the better detection capability. Moreover, this biosensor can be applicable to detect other biomarkers by using the appropriate antibodies. This biosensor has high potential for clinical diagnoses, personalized medicine and even environmental and food safety monitoring.

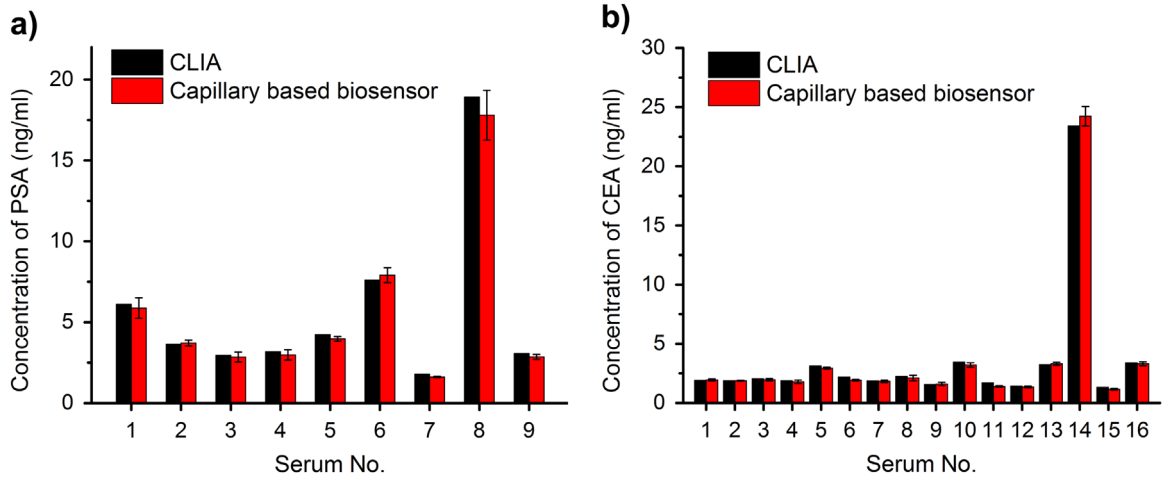

Fig. 5. Detection of PSA and CEA in serum samples. (a) The PSA assay results. (b) The CEA assay results.

Acknowledgements

This work was supported by the Guangdong Innovative and Entrepreneurial Research Team Program (201301S0105240297) and the Technology Research Program of Guangzhou City (201508020100).

Appendix A. Supplementary material

Supplementary data associated with this article can be found in the online version at http://dx.doi.org/10.1016/j.bios.2016.05.074.

References

Chen, Y., Wang, Y., Liu, L., Wu, X., Xu, L., Kuang, H., Li, A., Xu, C., 2015. Nanoscale 7 (39), 16381–16388.
Fu, Q., Liu, H.L., Wu, Z., Liu, A., Yao, C., Li, X., Xiao, W., Yu, S., Luo, Z., Tang, Y., 2015. J. Nanobiotechnol. 13 (1), 81.
Fu, Q., Tang, Y., Shi, C., Zhang, X., Xiang, J., Liu, X., 2013. Biosens. Bioelectron. 49, 399–402.
Gervais, L., De Rooij, N., Delamarche, E., 2011. Adv. Mater. 23 (24), H151–H176.
Ghannad-Rezaie, M., Wang, X., Mishra, B., Collins, C., Chronis, N., 2012. PLoS One 7, 1.
Hou, W., Wang, S., Wang, X., Han, X., Fan, H., Cao, S., Yue, J., Wang, Q., Jiang, W., Ding, C., 2015. PLoS One 10, 3.
Li, J.-F., Yang, Z.-L., Ren, B., Liu, G.-K., Fang, P.-P., Jiang, Y.-X., Wu, D.-Y., Tian, Z.-Q., 2006. Langmuir 22 (25), 10372–10379.
Li, X., Lu, D., Sheng, Z., Chen, K., Guo, X., Jin, M., Han, H., 2012. Talanta 100, 1–6.
Li, Y., Xuan, J., Xia, T., Han, X., Song, Y., Cao, Z., Jiang, X., Guo, Y., Wang, P., Qin, L., 2015. Anal. Chem. 87 (7), 3771–3777.
Liang, J., Liu, H., Lan, C., Fu, Q., Huang, C., Luo, Z., Jiang, T., Tang, Y., 2014. Nanotechnology 25 (49), 495501.
Liu, J., Lu, Y., 2006. Nat. Protoc.-Electron. Ed. 1 (1), 246.
Moody, M., Van, S., Arsdell, K., Orencole, S., Burns, C., 2001. Biotechniques 31 (1), 186–194.
Qin, C., Wen, W., Zhang, X., Gu, H., Wang, S., 2015. Analyst 140 (22), 7710–7717.
Shi, C.Y., Deng, N., Liang, J.J., Zhou, K.N., Fu, Q.Q., Tang, Y., 2015. Anal. Chim. Acta 854, 202–208.
Song, Y., Wang, Y., Qin, L., 2013. J. Am. Chem. Soc. 135 (45), 16785–16788.
Song, Y., Xia, X., Wu, X., Wang, P., Qin, L., 2014. Angew. Chem. 126 (46), 12659–12663.
Song, Y., Zhang, Y., Bernard, P.E., Reuben, J.M., Ueno, N.T., Arlinghaus, R.B., Zu, Y., Qin, L., 2012. Nat. Commun. 3, 1283.
Tanaka, T., Matsunaga, T., 2000. Anal. Chem. 72 (15), 3518–3522.
Tang, H., Chen, J., Nie, L., Kuang, Y., Yao, S., 2007. Biosens. Bioelectron. 22 (6), 1061–1067.
Urdea, M., Penny, L.A., Olmsted, S.S., Giovanni, M.Y., Kaspar, P., Shepherd, A., Wilson, P., Dahl, C.A., Buchsbaum, S., Moeller, G., 2006. Nature 444, 73–79.
Wang, H., Yuan, R., Chai, Y., Niu, H., Cao, Y., Liu, H., 2012. Biosens. Bioelectron. 37 (1), 6–10.
Zhu, Z., Guan, Z., Jia, S., Lei, Z., Lin, S., Zhang, H., Ma, Y., Tian, Z.Q., Yang, C.J., 2014. Angew. Chem. Int. Ed. 53 (46), 12503–12507.